EXPLAINING EXTREME EVENTS OF 2016

From A Climate Perspective

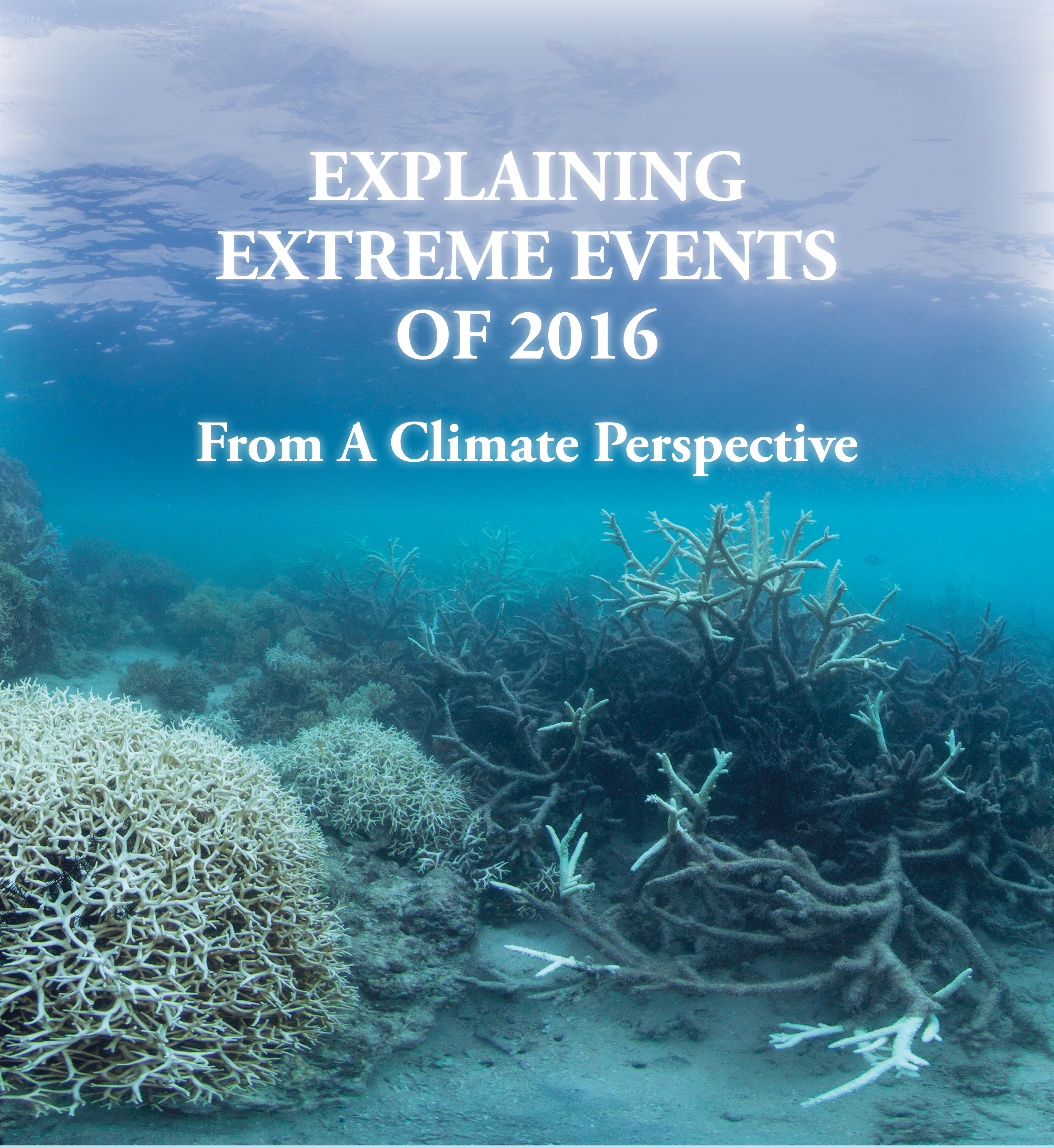

Special Supplement to the
Bulletin of the American Meteorological Society
Vol. 99, No. 1, January 2018

EXPLAINING EXTREME EVENTS OF 2016 FROM A CLIMATE PERSPECTIVE

Editors

Stephanie C. Herring, Nikolaos Christidis, Andrew Hoell, James P. Kossin,
Carl J. Schreck III, and Peter A. Stott

Special Supplement to the

Bulletin of the American Meteorological Society

Vol. 99, No. 1, January 2018

American Meteorological Society

Corresponding Editor:

Stephanie C. Herring, PhD
NOAA National Centers for Environmental Information
325 Broadway, E/CC23, Rm 1B-131
Boulder, CO 80305-3328
E-mail: stephanie.herring@noaa.gov

Cover credit:

HOW TO CITE THIS DOCUMENT

Citing the complete report:

Herring, S. C., N. Christidis, A. Hoell, J. P. Kossin, C. J. Schreck III, and P. A. Stott, Eds., 2018: Explaining Extreme Events of 2016 from a Climate Perspective. *Bull. Amer. Meteor. Soc.*, **99** (1), S1–S157.

Citing a section (example):

Quan, X.W., M. Hoerling, L. Smith, J. Perlwitz, T. Zhang, A. Hoell, K. Wolter, and J. Eischeid, 2018: Extreme California Rains During Winter 2015/16: A Change in El Niño Teleconnection? [in “Explaining Extreme Events of 2016 from a Climate Perspective”]. *Bull. Amer. Meteor. Soc.*, **99** (1), S54–S59, doi:10.1175/BAMS-D-17-0118.1.

EDITORIAL AND PRODUCTION TEAM

TABLE OF CONTENTS

Abstract ii

1. Introduction to Explaining Extreme Events of 2016 from a Climate Perspective 1
2. Explaining Extreme Ocean Conditions Impacting Living Marine Resources 7
3. CMIP5 Model-based Assessment of Anthropogenic Influence on Record Global Warmth During 2016 11
4. The Extreme 2015/16 El Niño, in the Context of Historical Climate Variability and Change 16
5. Ecological Impacts of the 2015/16 El Niño in the Central Equatorial Pacific 21
6. Forcing of Multiyear Extreme Ocean Temperatures that Impacted California Current Living Marine Resources in 2016 27
7. CMIP5 Model-based Assessment of Anthropogenic Influence on Highly Anomalous Arctic Warmth During November–December 2016 34
8. The High Latitude Marine Heat Wave of 2016 and Its Impacts on Alaska 39
9. Anthropogenic and Natural Influences on Record 2016 Marine Heat waves 44
10. Extreme California Rains During Winter 2015/16: A Change in El Niño Teleconnection? 49
11. Was the January 2016 Mid-Atlantic Snowstorm "Jonas" Symptomatic of Climate Change? 54
12. Anthropogenic Forcings and Associated Changes in Fire Risk in Western North America and Australia During 2015/16 60
13. A Multimethod Attribution Analysis of the Prolonged Northeast Brazil Hydrometeorological Drought (2012–16) 65
14. Attribution of Wintertime Anticyclonic Stagnation Contributing to Air Pollution in Western Europe 70
15. Analysis of the Exceptionally Warm December 2015 in France Using Flow Analogues 76
16. Warm Winter, Wet Spring, and an Extreme Response in Ecosystem Functioning on the Iberian Peninsula 80
17. Anthropogenic Intensification of Southern African Flash Droughts as Exemplified by the 2015/16 Season 86
18. Anthropogenic Enhancement of Moderate-to-Strong El Niño Events Likely Contributed to Drought and Poor Harvests in Southern Africa During 2016 91
19. Climate Change Increased the Likelihood of the 2016 Heat Extremes in Asia 97
20. Extreme Rainfall (R20mm, RX5day) in Yangtze–Huai, China, in June–July 2016: The Role of ENSO and Anthropogenic Climate Change 102
21. Attribution of the July 2016 Extreme Precipitation Event Over China's Wuhang 107
22. Do Climate Change and El Niño Increase Likelihood of Yangtze River Extreme Rainfall? 113
23. Human Influence on the Record-breaking Cold Event in January of 2016 in Eastern China 118
24. Anthropogenic Influence on the Eastern China 2016 Super Cold Surge 123
25. The Hot and Dry April of 2016 in Thailand 128
26. The Effect of Increasing CO_2 on the Extreme September 2016 Rainfall Across Southeastern Australia 133
27. Natural Variability Not Climate Change Drove the Record Wet Winter in Southeast Australia 139
28. A Multifactor Risk Analysis of the Record 2016 Great Barrier Reef Bleaching 144
29. Severe Frosts in Western Australia in September 2016 150
30. Future Challenges in Event Attribution Methodologies 155

ABSTRACT—Stephanie C. Herring, Nikolaos Christidi, Andrew Hoell, James P. Kossin, Carl J. Schreck III, and Peter A. Stott

This sixth edition of explaining extreme events of the previous year (2016) from a climate perspective is the first of these reports to find that some extreme events were not possible in a preindustrial climate. The events were the 2016 record global heat, the heat across Asia, as well as a marine heat wave off the coast of Alaska. While these results are novel, they were not unexpected. Climate attribution scientists have been predicting that eventually the influence of human-caused climate change would become sufficiently strong as to push events beyond the bounds of natural variability alone. It was also predicted that we would first observe this phenomenon for heat events where the climate change influence is most pronounced. Additional retrospective analysis will reveal if, in fact, these are the first events of their kind or were simply some of the first to be discovered.

Last year, the editors emphasized the need for additional papers in the area of "impacts attribution" that investigate whether climate change's influence on the extreme event can subsequently be directly tied to a change in risk of the socio-economic or environmental impacts. Several papers in this year's report address this challenge, including Great Barrier Reef bleaching, living marine resources in the Pacific, and ecosystem productivity on the Iberian Peninsula. This is an increase over the number of impact attribution papers than in the past, and are hopefully a sign that research in this area will continue to expand in the future.

Other extreme weather event types in this year's edition include ocean heat waves, forest fires, snow storms, and frost, as well as heavy precipitation, drought, and extreme heat and cold events over land. There were a number of marine heat waves examined in this year's report, and all but one found a role for climate change in increasing the severity of the events. While human-caused climate change caused China's cold winter to be less likely, it did not influence U.S. storm Jonas which hit the mid-Atlantic in winter 2016.

As in past years, the papers submitted to this report are selected prior to knowing the final results of whether human-caused climate change influenced the event. The editors have and will continue to support the publication of papers that find no role for human-caused climate change because of their scientific value in both assessing attribution methodologies and in enhancing our understanding of how climate change is, and is not, impacting extremes. In this report, twenty-one of the twenty-seven papers in this edition identified climate change as a significant driver of an event, while six did not. Of the 131 papers now examined in this report over the last six years, approximately 65% have identified a role for climate change, while about 35% have not found an appreciable effect.

Looking ahead, we hope to continue to see improvements in how we assess the influence of human-induced climate change on extremes and the continued inclusion of stakeholder needs to inform the growth of the field and how the results can be applied in decision making. While it represents a considerable challenge to provide robust results that are clearly communicated for stakeholders to use as part of their decision-making processes, these annual reports are increasingly showing their potential to help meet such growing needs.

11. WAS THE JANUARY 2016 MID-ATLANTIC SNOWSTORM "JONAS" SYMPTOMATIC OF CLIMATE CHANGE?

Klaus Wolter, Martin Hoerling, Jon K. Eischeid, and Dave Allured

Model simulations indicate that anthropogenic climate change has made extreme snowstorms less likely over the mid-Atlantic United States. Empirical evidence shows no decline since 1901, with recent storms colder than before.

Introduction. The biggest winter storm of 2016 named "Jonas"[1] over the eastern United States hit the mid-Atlantic states around 23 January, dumping up to 1 m of snow from Virginia to New York (Fig. 11.1a)[2], inflicting around $1 billion (U.S. dollars) in damages and causing 55 fatalities[3],[4].

This motivated our exploratory inquiry about how heavy winter precipitation events overall, and heavy snowstorms in particular, have changed in the mid-Atlantic region due to long-term climate change. In the eastern United States, heavy rain- and snowstorms have become more frequent during recent decades (Kunkel et al. 2013; Lawrimore et al. 2014). Both El Niño (Smith and O'Brien 2001; Lawrimore et al. 2014) and the negative phase of the NAO (Hoerling et al. 2010; Seager et al. 2010) increase the odds of heavy snow in this region. Given these natural drivers together with the regional rarity of major snowstorms (Changnon et al. 2006), identifying human-induced contributions requires model experimentation, results of which are presented here to augment empirical diagnosis of historical data.

Data and methods. A database of 987 climate stations (GHCN-D) of daily precipitation records since 1901 (Wolter et al. 2016) is used to identify heavy daily precipitation (≥25.4 mm). In the mid-Atlantic, 19 stations (Fig. 11.1b) have nearly complete records of precipitation, snowfall, and temperature during December–March 1900/01 through 2015/16. We define heavy daily snow (≥15.2 cm) in conjunction with heavy daily precipitation. Average temperatures during heavy precipitation days are used to derive an empirical relation of rain/snow transition thresholds for this region, inspired by Collins et al. (2004) and Kienzle (2008).

A 30-member ensemble of historical AMIP-style simulations is conducted with the T159 resolution (~85 km) ECHAM5 atmospheric model (Roeckner et al. 2003). This so-called "factual" simulation—using observed boundary and external radiative forcings—is compared to a parallel 30-member ensemble of "counterfactual" simulations. Linear trends of observed post-1880 sea surface temperatures (SST) are removed from the full time-varying SST; sea ice conditions are set to an early twentieth century climatology; and radiative forcings are altered to their 1880 values in counterfactual runs, thus retaining interannual and decadal variations of boundary forcings related to internal variability (Seager and Hoerling 2014; Sun et al. 2017, manuscript submitted to *Wea. Climate Extremes*). Simulated daily precipitation and temperature are analyzed for the mid-Atlantic domain of Fig. 11.1b. Heavy daily precipitation events are identified as in observations, and simulated snowstorms are inferred using the empirical relation of rain–snow temperature thresholds derived from observations. We compare factual versus counterfactual statistics of heavy precipitation and snowstorms for 2001–16 to maximize the climate change signal. A model's ability to simulate realistic storm tracks is an important attribute when considering heavy snowstorms. In this regard, we note

[1] http://nypost.com/2016/01/28/winter-storm-jonas-ranks-4th-worst-among-northeast-snowstorms/
[2] https://weather.com/storms/winter/news/winter-storm-jonas-record-snowstorm-new-york-city
[3] https://en.wikipedia.org/wiki/January_2016_United_States_blizzard
[4] www.washingtonpost.com/local/dc-politics/dcs-credit-card-was-shut-off-and-that-wasnt-the-worst-of-snowzilla-audit-finds/2017/01/11/5b84921a-d7f9-11e6-b8b2-cb5164beba6b_story.html?utm_term=.3c72de60003e&wpisrc=nl_localheads-draw6&wpmm=1

AFFILIATIONS: Wolter, Eischeid, and Allured—University of Colorado, Cooperative Institute for Research in Environmental Sciences and NOAA Earth System Research Laboratory, Boulder, Colorado; Hoerling—NOAA Earth System Research Laboratory, Boulder, Colorado

DOI:10.1175/BAMS-D-17-0130.1

A supplement to this article is available online (10.1175/BAMS-D-17-0130.2)

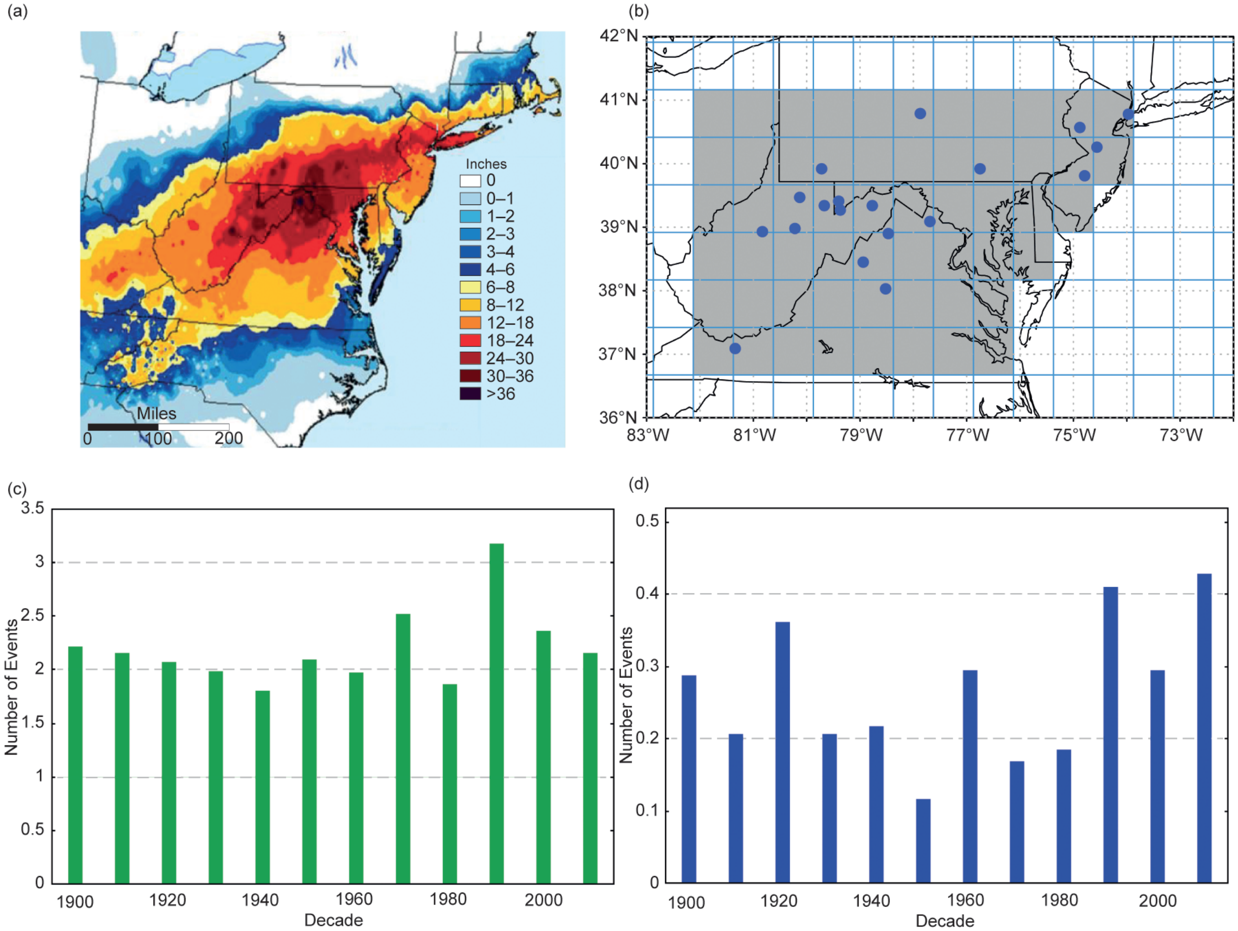

Fig. 11.1. (a) Jonas snowfall totals (inches); (b) 19 mid-Atlantic stations with 100yr+ precipitation records (Wolter et al. 2016) that also have more than 90% extant snowfall and temperature records during heavy precipitation days; gridding and shading refer to coverage by ECHAM5 for mid-Atlantic (~37°–41°N, ~74°–82°W); (c) Average annual counts of observed daily precipitation totals of 25.4 mm or higher from Dec–Mar 1900/01 through 2015/16 (last decade 2010/11 to 2015/16) for 19 mid-Atlantic stations; linear regression-based increase over 116 years: +20%; (d) As in (c) but for observed daily snowfall totals of 15.2 cm or higher (the number of usable stations varied from 16 to 19 per decade); linear regression-based increase over 116 years: +47%. [Source for (a): NWS Burlington.]

that storm tracks in the mid-Atlantic region are well represented in CMIP5 models with spatial resolution similar to that of our ECHAM5 experiments (Colle et al. 2015).

Results. (a) Empirical: Winter storm Jonas walloped our mid-Atlantic 19-station network: 12 stations reported daily totals of at least 23 cm of snow (25.4 mm of precipitation); see online supplement for more details.

Figure 11.1c documents the average number of heavy precipitation days per winter season and station on a decadal basis (overall average: 2.2). Figure 11.1d does the same for heavy snow days (average: 0.26). While both time series show an increase over the last 12 decades, their linear trends are not statistically significant due to large decadal variability. Nevertheless, our results for the mid-Atlantic corroborate upward trends in heavy snowstorms since 1901 in the Northeast (Kunkel et al. 2013).

When binned by daily average temperatures (Tave; Table 11.1), heavy precipitation events above +2°C contain little snow [snow-to-rain ratio (S/R) < 1], while those below −6°C guarantee heavy snow days (S/R > 8). We calculated heavy snow water equivalent (SWE; 15.2 mm) days based on assuming that no snow fell above +2°C, all snow below −6°C, and linear fractions in-between. This is similar to Collins et al. (2004) who inferred snowfall in the NCAR CAM3 model using 0°C and −5°C for their all-rain and all-snow thresholds. For the 19 mid-Atlantic stations, a total of 518 calculated heavy SWE days correspond well to 538 observed heavy snow days since 1901.

Table 11.1. Nineteen mid-Atlantic stations with more than 90% daily data for Dec–Mar 1900/01–2015/16, focusing on heavy daily precipitation events (25.4 mm+). "Tave" refers to daily average temperature bins (in 1°C steps between +6°C and −6°C); "#rain" refers to total number of rain-only events; "#snow" lists total number of heavy precipitation events with more than trace of snow; "%snow" gives percentage of the snowy days to total count [#snow*100/(#rain+#snow)]; "<S/R>" refers to total amount of snow divided by total amount of precipitation in each temperature bin; and "%6+:1" refers to percentage of snowy days with snow:rain ratio of 6:1 or higher. In each column, biggest values are highlighted in green, lowest in red.

Tave (°C)	#rain	#snow	%snow	<S/R>	%6+:1
≥6°C	1783	43	2.4%	0.05	0.1%
≥5/<6	372	33	8.1	0.17	0.7
≥4/<5	256	38	12.9	0.26	1.0
≥3/<4	324	67	17.1	0.36	1.5
≥2/<3	208	88	29.7	0.77	3.7
≥1/<2	203	127	38.5	1.21	5.8
≥0/<1	119	177	59.8	2.51	15.9
≥−1/<0	060	117	66.1	2.85	20.8
≥−2/<−1	036	173	82.8	4.06	30.6
≥−3/<−2	017	093	84.5	4.88	40.0
≥−4/<−3	018	094	83.9	5.48	45.6
≥−5/<−4	012	054	81.8	5.41	45.5
≥−6/<−5	005	031	86.1	7.28	61.1
<−6°C	003	117	97.5%	8.14	69.2%

Heavy snow counts show *no significant* change since 1901. Surprisingly, heavy snow days have become *significantly colder* (−2.55°C), in contrast with heavy rain-only days which have warmed slightly (+0.35°C; both in Fig. ES11.1).

(b) Model: Figure 11.2 shows results for the mid-Atlantic region from our model simulations. The Dec–Mar temperature difference between the factual and counterfactual experiments is +0.84°C (Fig. 11.2a) which is lower than the observed trend since 1900 (+1.1°C; Fig. ES11.2a). The corresponding precipitation difference for the same set of runs shows little change (+0.2%; Fig. 11.2b), compared to an observed decline of −4% (Fig. ES11.2b).

For each grid box and ensemble member, heavy precipitation events are extracted for Dec–Mar 2000/01 through 2015/16. Consistent with a wet bias of the model, the average number of such events is 3.7 per grid box in the factual case (Fig. 11.2c), *higher* than the observed frequency per climate station (2.3; Fig. 11.1c). Model snowstorms are derived by applying the same algorithm to calculate SWE as for observed data. The number of simulated heavy snow days is 0.17 cases per winter and grid box in the factual case (Fig. 11.2d), *lower* than observed (0.34; Fig. 11.1d).

Given the large model sample size, we find statistically significant changes in the frequency of heavy precipitation and snow days as a consequence of long-term climate change. An *increase* in the average number of heavy precipitation days of 7.0% is 99% significant for the means, but not for the full distribution [Fig. 11.2c; Komolgorov–Smirnov (K–S) value of 0.13]. A *decrease* by 17.5% for the average number of heavy snow days (Fig. 11.2d) is significant (*t*-test: 99%; K–S = 0.07). Comparing the number of events per winter in factual versus counterfactual climates indicates that 68.5% of the factual precipitation seasons exceed the counterfactual median (3.5 events per winter; Fig. 11.2c), a 37% increase in the relative risk of heavy precipitation events. By contrast, for heavy snowstorms, only 24.1% of the factual model seasons exceed the counterfactual median (0.2 events per winter; Fig. 11.2d), a 52% decrease in the relative risk of heavy snowstorms. Thus, the modeled likelihood of experiencing a heavy snowstorm has decreased in recent decades, as a result of climate change alone.

Comparing the probability distributions of both factual and counterfactual runs shows a wide spread in outcomes for heavy precipitation and snow events (Fig. 11.2c,d). This suggests low confidence in detecting the forced signal from a single sample of historical data. Concerning the model's forced signal,

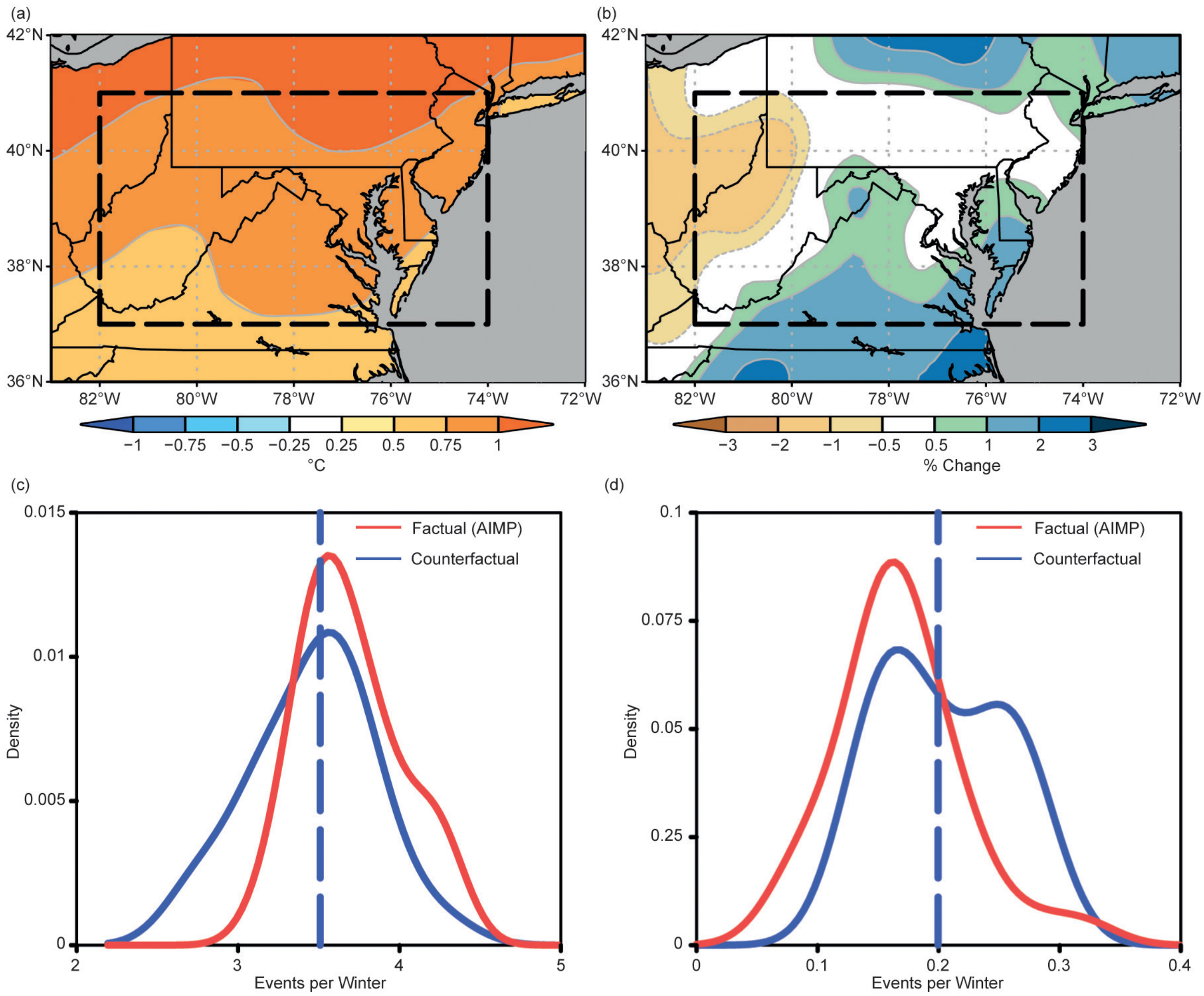

FIG. 11.2. ECHAM5 output for Dec–Mar 2000/01 through 2015/16. (a) Map of average change in seasonal temperatures (°C) of 30 factual runs compared to 30 counterfactual runs (+0.84°C) for mid-Atlantic (stippled outline); (b) As in (a) but for seasonal precipitation (+0.2%); (c) Probability distributions for mid-Atlantic region (57 grid boxes in Fig. 11.1b) for daily precipitation totals ≥ 25.4 mm, with median of 3.5 such events per season and grid box in counterfactual case (blue stippled vertical line); (d) As in (c) but for heavy snow events (SWE ≥ 15.2 mm), with median of 0.20 such events per counterfactual season and grid box. Probability distributions are nonparametric estimates of frequency distributions based on Kernel density and have been smoothed using Gaussian filter.

a key ingredient in its decrease of heavy snowstorms must be its increase in average temperature during modeled heavy precipitation days. More frequent heavy precipitation events alone—a plausible symptom of increased water vapor in a warmer climate (Hartmann et al. 2014)—would have implied more snowstorms. However, an increase in temperature more than countervailed the increase in moisture, yielding less heavy snowstorms.

Concluding remarks. Jonas was one of the most severe mid-Atlantic snowstorms of the last century (see http://nypost.com/2016/01/28/winter-storm-jonas-ranks-4th-worst-among-northeast-snowstorms/). We address how a class of such storms rather than Jonas itself are affected by anthropogenic climate change. Heavy snowstorm statistics derived from parallel climate experiments, one subjected to current climate conditions, the other subjected to conditions of the late nineteenth century, indicate a 52% decrease in the relative risk of experiencing a heavy snowstorm. Warmer temperatures dominated over the occurrence of more frequent heavy precipitation events in the model leading to fewer heavy snowstorms in the current climate. By contrast, the long-term observational record shows more heavy snowstorms in recent decades.

We reconcile these differences between the modeled and observed changes in heavy snowstorms by noting the large spread among the 30-members of ECHAM5 simulated mid-Atlantic snowstorm changes, implying low detectability of a change signal at this time. Heavy snowstorms are rare in the mid-Atlantic region, and their probability is affected by various natural drivers (El Niño, atmospheric blocking). Recent mid-Atlantic snowstorms were colder than those of the earlier twentieth century, contrary to a general winter warming trend in the region. It is plausible that internal variations in weather patterns responsible for mid-Atlantic snowstorms have dominated the observed increase. For instance, an eastward shift of storm tracks to slightly more offshore could cool the air mass during heavy precipitation events, allowing for heavy snow to fall over a wider reach of the mid-Atlantic (Changnon et al. 2008). In this regard, our results show a temperature increase of +0.3°C during model snowstorms, in contrast with the cooling trend in observed snowstorms since 1901 (−2.55°C), which may be due to natural decadal variations in storm tracks.

We further speculate that the wide observed range of temperatures during heavy snowstorms, many of them colder than −6°C, should allow for a continuation of at least some heavy snowstorm activity well into the future. This is consistent with O'Gorman's (2014) projection of only a slight decrease in the frequency of future extreme snowstorms compared to a much bigger decrease in seasonal snowfall totals for much of the northern midlatitudes. Meanwhile, the number of heavy mid-Atlantic snowstorms during the month of March has indeed declined compared to previous decades (Table ES11.1). Perhaps the future is showing its hand after all.

ACKNOWLEDGMENTS. Three anonymous reviews and comments by Jeff Rosenfeld (editor) helped to improve our manuscript.

REFERENCES

Changnon, D., C. Merinsky, and M. Lawson, 2008: Climatology of surface cyclone tracks associated with large central and eastern U.S. snowstorms, 1950–2000. *Mon. Wea. Rev.*, **136**, 3193-3202, doi:10.1175/2008MWR2324.1.

Changnon, S. A., D. Changnon, and T. R. Karl, 2006: Temporal and spatial characteristics of snowstorms in the contiguous United States. *J. Appl. Meteor. Climatol.,* **45**, 1141–1155, doi:10.1175/JAM2395.1.

Colle, B. A., J. F. Booth, and E. K. M. Chang, 2015: A review of historical and future changes of extratropical cyclones and associated impacts along the U.S. east coast. *Curr. Climate Change Rep.,* **1**, 125-143, doi:10.1007/s40641-015-0013-7.

Collins, W. D., and Coauthors, 2004: Description of the NCAR Community Atmosphere Model (CAM3). NCAR Tech. Rep. NCAR/TN-464+STR, 226 pp. (Available online at www.ccsm.ucar.edu/models/atm-cam/docs/description/description.pdf.)

Hartmann, D. L., and Coauthors, 2014: Observations: Atmosphere and surface. *Climate Change 2013: The Physical Basis.* T. F. Stocker et al., Eds., Cambridge University Press, 159–254.

Hoerling, M., and Coauthors, 2010: Understanding the Mid-Atlantic snowstorms during the winter of 2009-2010. NOAA-ESRL, 16 pp. [Available online at www.esrl.noaa.gov/psd/csi/images/NOAA_AttributionTeam_SnowstormReport.pdf.]

Kienzle, S. W., 2008: A new temperature based method to separate rain and snow. *Hydrol. Process.*, **22**, 5067–5085, doi:10.1002/hyp.7131.

Kunkel, K. E., and Coauthors, 2013: Monitoring and understanding trends in extreme storms: State of knowledge. *Bull. Amer. Meteor. Soc.*, **94**, 499–514, doi:10.1175/BAMS-D-11-00262.1.

Lawrimore, J., T. R. Karl, M. Squires, D. A. Robinson, and K. E. Kunkel, 2014: Trends and variability in severe snowstorms east of the Rocky Mountains. *J. Hydrometeor.*, **15**, 1762–1777, doi:10.1175/JHM-D-13-068.1.

O'Gorman, P. A. 2014: Contrasting responses of mean and extreme snowfall to climate change. *Nature,* **512**, 416–418, doi:10.1038/nature13625.

Roeckner, E. K., and Coauthors, 2003: The atmospheric general circulation model ECHAM5. Part I: Model description. MPI Tech. Rep. 349, 127 pp. [Available online at www.mpimet.mpg.de/fileadmin/publikationen/Reports/max_scirep_349.pdf.]

Seager, R., and M. Hoerling, 2014: Atmosphere and ocean origins of North American droughts. *J. Climate,* **27**, 4581–4606, doi:10.1175/JCLI-D-13-00329.1.

——, Y. Kushnir, J. Nakamura, M. Ting, and M. Naik, 2010: Northern Hemisphere winter snow anomalies: ENSO, NAO, and the winter of 2009/10. *Geophys. Res. Lett*., **37**, L14703, doi:10.1029/2010GL043830.

Smith, S. R., and J. J. O'Brien, 2001: Regional snowfall distributions associated with ENSO: Implications for seasonal forecasting. *Bull. Amer. Meteor. Soc*., **82**, 1179–1191.

Wolter, K., M. Hoerling, J. K. Eischeid, and L. Cheng, 2016: What history tells us about 2015 U.S. daily rainfall extremes [in "Explaining Extreme Events of 2015 from a Climate Perspective"]. *Bull. Amer. Meteor. Soc*., **97** (12), S9–S13, doi:10.1175/BAMS-D-16-0166.1.

Table 1.1. SUMMARY of RESULTS

	ANTHROPOGENIC INFLUENCE ON EVENT		
	INCREASE	**DECREASE**	**NOT FOUND OR UNCERTAIN**
Heat	Ch. 3: Global Ch. 7: Arctic Ch. 15: France Ch. 19: Asia		
Cold		Ch. 23: China Ch. 24: China	
Heat & Dryness	Ch. 25: Thailand		
Marine Heat	Ch. 4: Central Equatorial Pacific Ch. 5: Central Equatorial Pacific Ch. 6: Pacific Northwest Ch. 8: North Pacific Ocean/Alaska Ch. 9: North Pacific Ocean/Alaska Ch. 9: Australia		Ch. 4: Eastern Equatorial Pacific
Heavy Precipitation	Ch. 20: South China Ch. 21: China (Wuhan) Ch. 22: China (Yangtze River)		Ch. 10: California (failed rains) Ch. 26: Australia Ch. 27: Australia
Frost	Ch. 29: Australia		
Winter Storm			Ch. 11: Mid-Atlantic U.S. Storm "Jonas"
Drought	Ch. 17: Southern Africa Ch. 18: Southern Africa		Ch. 13: Brazil
Atmospheric Circulation			Ch. 15: Europe
Stagnant Air			Ch. 14: Western Europe
Wildfires	Ch. 12: Canada & Australia (Vapor Pressure Deficits)		
Coral Bleaching	Ch. 5: Central Equatorial Pacific Ch. 28: Great Barrier Reef		
Ecosystem Function		Ch. 5: Central Equatorial Pacific (Chl-***a*** and primary production, sea bird abundance, reef fish abundance) Ch. 18: Southern Africa (Crop Yields)	
El Niño	Ch. 18: Southern Africa		Ch. 4: Equatorial Pacific (Amplitude)
TOTAL	18	3	9

	METHOD USED	Total Events
Heat	Ch. 3: CMIP5 multimodel coupled model assessment with piCont, historicalNat, and historical forcings Ch. 7: CMIP5 multimodel coupled model assessment with piCont, historicalNat, and historical forcings Ch. 15: Flow analogues conditional on circulation types Ch. 19: MIROC-AGCM atmosphere only model conditioned on SST patterns	
Cold	Ch. 23: HadGEM3-A (GA6) atmosphere only model conditioned on SST and SIC for 2016 and data fitted to GEV distribution Ch. 24: CMIP5 multimodel coupled model assessment	
Heat & Dryness	Ch. 25: HadGEM3-A N216 Atmosphere only model conditioned on SST patterns	
Marine Heat	Ch. 4: SST observations; SGS and GEV distributions; modeling with LIM and CGCMs (NCAR CESM-LE and GFDL FLOR-FA) Ch. 5: Observational extrapolation (OISST, HadISST, ERSST v4) Ch. 6: Observational extrapolation; CMIP5 multimodel coupled model assessment Ch. 8: Observational extrapolation; CMIP5 multimodel coupled model assessment Ch. 9: Observational extrapolation; CMIP5 multimodel coupled model assessment	
Heavy Precipitation	Ch. 10: CAM5 AMIP atmosphere only model conditioned on SST patterns and CESM1 CMIP single coupled model assessment Ch. 20: Observational extrapolation; CMIP5 and CESM multimodel coupled model assessment; auto-regressive models Ch. 21: Observational extrapolation; HadGEM3-A atmosphere only model conditioned on SST patterns; CMIP5 multimodel coupled model assessment with ROF Ch. 22: Observational extrapolation, CMIP5 multimodel coupled model assessment Ch. 26: BoM seasonal forecast attribution system and seasonal forecasts Ch. 27: CMIP5 multimodel coupled model assessment	
Frost	Ch. 29: *weather@home* multimodel atmosphere only models conditioned on SST patterns; BoM seasonal forecast attribution system	
Winter Storm	Ch. 11: ECHAM5 atmosphere only model conditioned on SST patterns	
Drought	Ch. 13: Observational extrapolation; weather@home multimodel atmosphere only models conditioned on SST patterns; HadGEM3-A and CMIP5 multimodel coupled model assessent; hydrological modeling Ch. 17: Observational extrapolation; CMIP5 multimodel coupled model assessment; VIC land surface hdyrological model, optimal fingerprint method Ch. 18: Observational extrapolation; *weather@home* multimodel atmosphere only models conditioned on SSTs, CMIP5 multimodel coupled model assessment	
Atmospheric Circulation	Ch. 15: Flow analogues distances analysis conditioned on circulation types	
Stagnant Air	Ch. 14: Observational extrapolation; Multimodel atmosphere only models conditioned on SST patterns including: HadGEM3-A model; EURO-CORDEX ensemble; EC-EARTH+RACMO ensemble	
Wildfires	Ch. 12: HadAM3 atmospere only model conditioned on SSTs and SIC for 2015/16	
Coral Bleaching	Ch. 5: Observations from NOAA Pacific Reef Assessment and Monitoring Program surveys Ch. 28: CMIP5 multimodel coupled model assessment; Observations of climatic and environmental conditions (NASA GES DISC, HadCRUT4, NOAA OISSTV2)	
Ecosystem Function	Ch. 5: Observations of reef fish from NOAA Pacific Reef Assessment and Monitoring Program surveys; visual observations of seabirds from USFWS surveys. Ch. 18: Empirical yield/rainfall model	
El Niño	Ch. 4: SST observations; SGS and GEV distributions; modeling with LIM and CGCMs (NCAR CESM-LE and GFDL FLOR-FA) Ch. 18: Observational extrapolation; *weather@home* multimodel atmosphere only models conditioned on SSTs, CMIP5 multimodel coupled model assessment	
		30